Column-supported hyperboloids under wind loading

Autor(en): **Gould, Phillip L. / Lee, Seng-Lip**

Objekttyp: **Article**

Zeitschrift: **IABSE publications = Mémoires AIPC = IVBH Abhandlungen**

Band (Jahr): **31 (1971)**

PDF erstellt am: **16.08.2024**

Persistenter Link: https://doi.org/10.5169/seals-24218

Column-Supported Hyperboloids Under Wind Loading

L'hyperboloide reposant sur piliers sous les charges du vent

Durch Stützen getragene Hyperboloide unter Windlast

PHILLIP L. GOULD
Associate Professor of Civil Engineering
Washington University, St. Louis,
Missouri

SENG-LIP LEE
Professor of Civil Engineering, Asian
Institute of Technology, Bangkok,
Thailand

Introduction

A hyperboloid of revolution supported by a ring beam and a large number of closely spaced columns, as shown in Fig. 1, is commonly used as a natural draught, reinforced concrete cooling tower. An analysis of a column-supported hyperboloid subject to gravity loading has been presented elsewhere [5], and a review of the literature treating symmetrically loaded shells of revolution with discrete supports is contained therein. In addition, STEELE [11] and ELMS [1] have examined the effects of self-equilibrated edge loading on this class of shells. The wind load considered in this paper, shown in Fig. 2, is a quasistatic design wind load based on the results of wind tunnel tests [10]. Many other pressure distributions have been discussed in the literature including prototype measurements [7] and all are amenable to this analysis when represented in harmonic form.

The objectives of the present investigation are [I] to generalize the previously developed solution [5], which is valid only for large values of the harmonic number n, so that it is applicable for all values of $n > 1$; and [II] to use this solution, in conjunction with the available continuous boundary solutions [3], [4], [6], to analyze a column-supported hyperboloid of revolution under the design wind loading.

In order to clarify these objectives, it is necessary to examine the idealization proposed for the lower boundary of the shell. As shown in Fig. 3a the meridional stress N_ϕ is assumed to be uniformly distributed over the width of the column. The intensities of the distributed reactions are determined from a

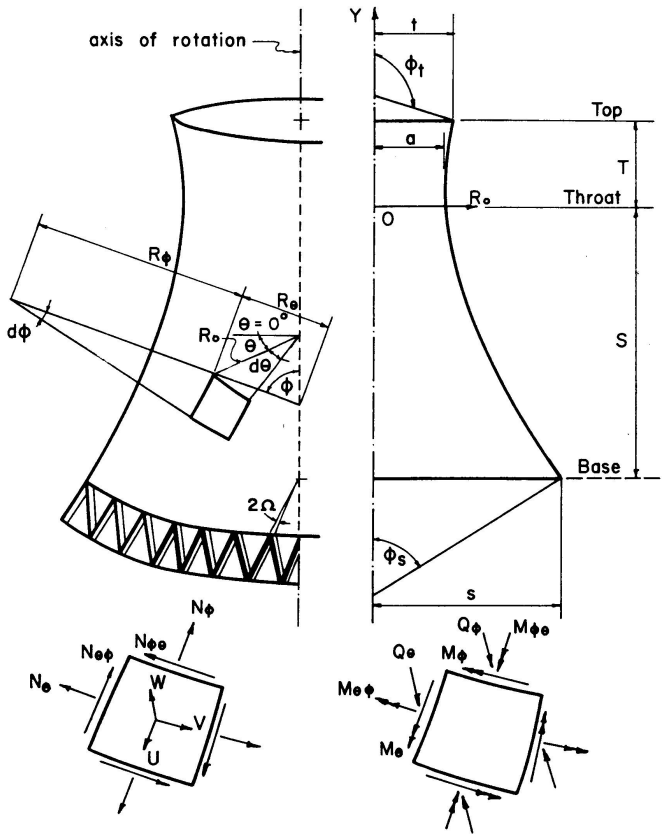

Fig. 1. Hyperboloid of Revolution.

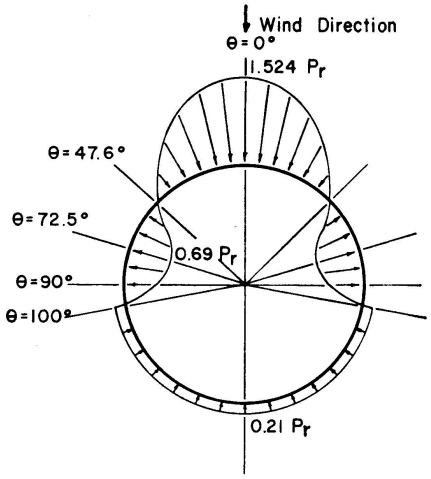

Fig. 2. Design Wind Pressure.

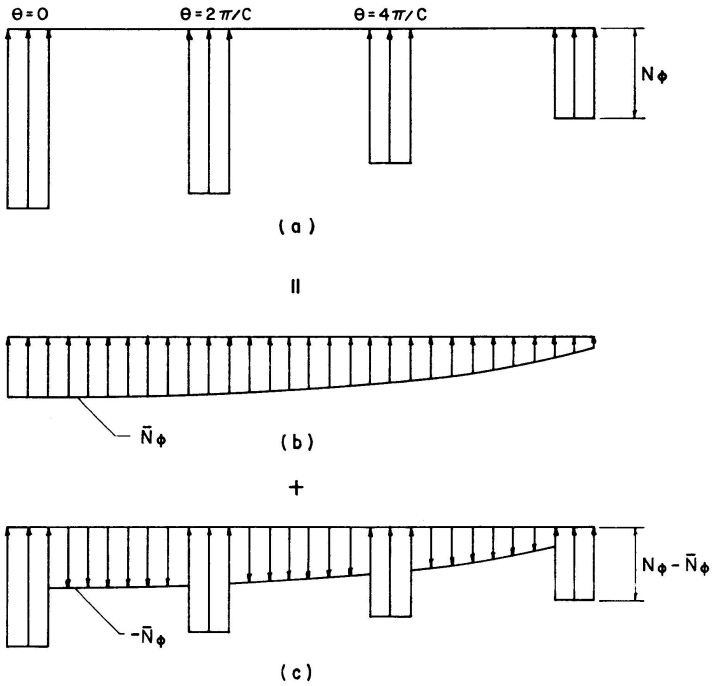

Fig. 3. Superposition Representation of Column Reactions.

continuous boundary analysis by computing the force tributary to each column and dividing by the column width. This idealized support system is represented by a superposition of the continuous boundary reaction, shown

in Fig. 3b and a self-equilibrated edge load, shown in Fig. 3c, which is composed of the negative of the continuous boundary reaction between columns and the difference between the uniformly distributed column reaction and the negative continuous boundary reaction within the column width. When this edge loading is represented by a Fourier series, all harmonics participate except $n=0$ and $n=1$ which are not self-equilibrating but must correspond to an external loading [2]. This is in contrast to the solution for gravity loading in which symmetry restricts the participation to harmonics which are integer multiples of the total number of columns [2], [4]. Therefore, it is necessary that the solution employed in Ref. [5] be generalized to include all harmonics $n>1$.

Surface Geometry

The geometry of a hyperboloid of revolution, shown in Fig. 1, is defined by

$$r_0^2-(k^2-1)\,y^2=1, \tag{1a}$$

in which

$$r_0=\frac{R_0}{a}, \qquad y=\frac{Y}{a}, \qquad k^2=1+\frac{a^2}{b^2} \tag{1b}$$

and R_0 = the horizontal radius, Y = the vertical coordinate, a = the throat radius and

$$b=\frac{a\,T}{\sqrt{t^2-a^2}}=\frac{a\,S}{\sqrt{s^2-a^2}}, \tag{1c}$$

in which s = the base radius, t = the top radius, and S and T = the vertical distances from the throat to the base and the top of the shell, respectively.

The coordinate system is also shown in Fig. 1 where the positive directions of ϕ and θ are indicated. The angles ϕ_s and ϕ_t denote the base and top of the shell, respectively, and

$$R_\theta=a\,r_\theta=\frac{\sqrt{k^2-1}}{\sqrt{k^2\sin^2\phi-1}}, \qquad R_\phi=a\,r_\phi=\frac{-a\sqrt{k^2-1}}{(k^2\sin^2\phi-1)^{3/2}}, \tag{2a, b}$$

in which r_θ and r_ϕ are the nondimensional principal radii of curvature. Also, H denotes the constant thickness of the shell and 2Ω the angle subtended by the column measured in the horizontal plane. The shell is geometrically described by the dimensionless parameters a/s, a/t, H/a, k and the throat radius a.

It is convenient to define the geometric parameter

$$\delta=\left(\frac{1}{r_\phi}-\frac{1}{r_\theta}\right)csc^2\phi. \tag{3}$$

For the hyperboloid, in view of Eqs. (2a) and (2b),

$$\delta=-\frac{k^2}{r_\theta}. \tag{4}$$

Governing Equations

Derivation and Definitions

The formulation is based on the Novozhilov equations in terms of stress resultants which combine the bending theory equilibrium equations for thin shells of revolution and the Gol'denveizer compatibility relationships [5], [8]. The stress resultants used in the formulation, shown in Fig. 1, are nondimensionalized as

$$\{R\} = \{n_\phi\, n_\theta\, n_{\theta\phi}\, m_\phi\, m_\theta\, m_{\theta\phi}\, q_\phi\, q_\theta\} = \frac{1}{a^2}\{N_\phi\, N_\theta\, N_{\theta\phi}\, M_\phi a\, M_\theta a\, M_{\theta\phi} a\, Q_\phi\, Q_\theta\} \tag{5a}$$

and taken in the form

$$\{R\} = \sum_{n=0}^{\infty} [\Theta]\{R_n\}, \tag{5b}$$

in which $\{R_n\} = \{n_{\phi n}\, n_{\theta n}\, n_{\theta\phi n}\, m_{\phi n}\, m_{\theta n}\, m_{\theta\phi n}\, q_{\phi n}\, q_{\theta n}\}$

and $[\Theta] = [\cos n\theta \cos n\theta \sin n\theta \cos n\theta \cos n\theta \sin n\theta \cos n\theta \sin n\theta]$.

Transformation of Equations

In order to uncouple the Novozhilov equations, the parameter δ, as given by Eqs. (3) and (4), must be a constant [8]. Although not strictly true for a hyperboloid, δ will be approximated by a constant $\delta(\phi_s)$ where ϕ_s denotes the base of the shell as shown in Fig. 1. This approximation is based on the assumption that the edge effects are rapidly attenuating from the base of the shell, which has been shown to be valid for gravity loading [5].

Taking
$$\delta \cong \frac{-k^2}{s\,c\,s\,c\,\phi_s} \tag{6}$$

the homogeneous Novozhilov equations for harmonic n take the form [5], [8]

$$\frac{d^2\xi_j}{d\phi^2} - F_j^2\,\xi_j = 0, \quad (j = 1, 2), \tag{7}$$

in which ξ_1 and ξ_2 = complex auxiliary variables defined elsewhere [5]

$$F_j^2 = -\frac{i}{\nu}\frac{r_\phi^2}{2\,r_\theta}[1 \pm \sqrt{1 - 4\,i\,n^2\,\nu\,\delta - 4\,n^2\,(\nu\,\delta)^2}] + \left(\frac{n\,r_\phi}{r_\theta \sin\phi}\right)^2$$
$$-\frac{1}{2\,r_\phi}\frac{d^2 r_\phi}{d\phi^2} + \frac{3}{4\,r_\phi^2}\left(\frac{dr_\phi}{d\phi}\right)^2 + \frac{\cot\phi}{2\,r_\phi}\frac{dr_\phi}{d\phi} - \frac{r_\phi}{r_\theta \sin^2\phi} + \frac{2 + \cos^2\phi}{4\sin^2\phi},$$

$$\nu = \frac{h}{\sqrt{12\,(1-\mu^2)}}$$

and μ = Poisson's ratio.

The upper and lower signs correspond to $j = 1,2$ respectively.

At this point, the treatment must be generalized from that presented in Ref. [5] which was based on the recognition that only harmonics which are integer multiples of the total number of columns participate in the solution for symmetric loading. For the asymmetric loading considered in this paper, the solution must be valid for all $n > 1$ necessitating the retention of certain terms which were dropped in the previous treatment. The reason for eliminating harmonics $n = 0$ and $n = 1$ from consideration in this solution was stated in the introduction.

The first term of F_j is $0(r_\phi)$, the second $0(n^2)$ and the remainder $0(1)$. Furthermore the term $4n^2(\nu\delta)^2$ under the radical is negligible compared to $4n^2\nu\delta$. Dropping small quantities leads to

$$F_j = -\overline{W}_j^{0.25} e^{i\gamma_j}\left(\frac{r_\phi}{\sqrt{r_\theta \nu}}\right), \quad (j = 1, 2), \tag{8}$$

in which

$$\begin{aligned}
W_j &= 0.25 \pm 0.5\, W_0 \cos\gamma_0 \pm \frac{n^2\nu}{r_\theta \sin^2\phi} W_0 \sin\gamma_0 + \frac{n^4\nu^2}{r_\theta^2 \sin^4\phi} + 0.25\, W_0^2, \\
\gamma_j &= 0.5 \tan^{-1}\bar{\gamma}_j, \\
\bar{\gamma}_j &= \frac{-r_\theta \sin^2\phi\,(1 \pm W_0 \cos\gamma_0)}{2\nu n^2 \pm r_\theta \sin^2\phi\, W_0 \sin\gamma_0}, \\
W_0 &= [1 + 16 n^4 (\nu\delta)^2]^{0.25}, \\
\gamma_0 &= 0.5 \tan^{-1}(-4n^2\nu\delta).
\end{aligned}$$

Solution of Governing Equations

The solution to Eq. (7), obtained by asymptotic integration, is [3], [8]

$$\xi_j = \frac{1}{\sqrt{F_j}}(\tilde{C}_{1j} e^{\beta_j} + \tilde{C}_{2j} e^{-\beta_j}), \tag{9}$$

in which $$\beta_j = \int F_j \, d\phi$$

and $\tilde{C}_{1j}$ and $\tilde{C}_{2j}$ are complex integration constants.

Once the solution to Eq. (9) is obtained, the complex auxiliary variables defined in the formulation may be decomposed into real and imaginary parts and suitably combined to give explicit expressions for the stress resultants defined in Eq. (5). The details of these transformations are given elsewhere [5]. After considerable algebraic manipulation the stress resultants for harmonic n may be arranged in the form

$$\{R_n\} = [B][D_1][D_2][\bar{U}]\{C\}, \tag{10}$$

in which $\{R_n\}$ is given by Eq. (5b) and the elements of matrices B, D_1, D_2, $\bar{U}$ and C are specified in Appendix 1. The resulting expressions for the stress resultants are similar to those presented earlier [5] appropriately amended by the incorporation of the generalizations introduced in this paper to extend the theory to include the lower harmonics.

Application of Solution

Discrete Support System

As described in the introduction, the discrete support system is assumed to be represented by the superposition shown in Fig. 3. The continuous support system shown in Fig. 3b is best solved using the homogeneous solution given elsewhere [3] and taking the particular solution as the membrane theory solution [4]. The self-equilibrated system shown in Fig. 3c is solved using the expressions derived in this paper.

Assuming that the column reactions are uniformly distributed over the width of the columns with total magnitude equal to the tributary continuous boundary reaction, the intensity of the column reaction $\bar{R}_\lambda$ for a column with center line at $\theta = \theta_\lambda$ is given by

$$\bar{R}_\lambda = \frac{1}{2\Omega} \int_{\theta_\lambda - (\pi/c)}^{\theta_\lambda + (\pi/c)} \bar{n}_\phi (\phi_s, \theta)\, d\theta, \tag{11}$$

in which c = the total number of equally spaced column support points,
$\bar{n}_\phi$ = the continuous boundary reaction,
$\theta_\lambda = \frac{2\pi\lambda}{c}$
and λ = the column number $(0, 1, \ldots, c-1)$.

The continuous boundary reaction $\bar{n}_\phi (\phi_s, \theta)$ is given by

$$\bar{n}_\phi = \sum_{n=0}^{\infty} \bar{n}_{\phi n} (\phi_s) \cos n\theta, \tag{12}$$

where the expressions for $\bar{n}_{\phi n}$ are given elsewhere [3], [4], [6]. It should be noted that Eq. (12) represents the meridional stress resultant at the base of the shell as shown in Fig. 3b. Substituting Eq. (12) into Eq. (11) and integrating yields

$$\bar{R}_\lambda = \bar{n}_{\phi 0} \frac{\pi}{c\Omega} + \frac{1}{\Omega} \sum_{n=1}^{\infty}{}' \bar{n}_{\phi n} (\phi_s) \sin \frac{n\pi}{c} \frac{\cos n\theta_\lambda}{n}. \tag{13}$$

The stress resultant distribution shown in Fig. 3c is given by the negative of Eq. (12) between columns and the difference between Eqs. (13) and (12) within each column width. In order to represent this mathematically, it is convenient to expand the system of c column reactions, each of which may be evaluated by substituting the appropriate value of θ_λ in Eq. (13), into a Fourier series. To be consistent with the assumption of a uniformly distributed column reaction, prior to expanding Eq. (13) in Fourier series $\bar{R}_\lambda$ is evaluated explicitly at each column λ with the series contained in Eq. (13) truncated at the same value of n which produces acceptable accuracy for the computation of $\bar{n}_\phi$ in Eq. (12).

The Fourier cosine coefficients for the c column reactions are given by

$$\bar{n}'_{\phi n} = \frac{1}{\pi} \sum_{\lambda=0}^{\lambda=c-1} \int_{(2\pi\lambda/c)-\Omega}^{(2\pi\lambda/c)+\Omega} \bar{R}_\lambda \cos n\theta \, d\theta = \frac{2}{\pi} \sum_{\lambda=0}^{\lambda=c-1} \bar{R}_\lambda \cos \frac{2\pi n\lambda}{c} \frac{\sin n\Omega}{n}, \quad (n>1) \tag{14}$$

and the support condition shown in Fig. 3c is represented by

$$n_\phi(\phi_s) = \sum_{n=2}^{\infty} \bar{n}''_{\phi n}(\phi_s) \cos n\theta, \tag{15}$$

in which

$$\bar{n}''_{\phi n}(\phi_s) = \bar{n}'_{\phi n} - \bar{n}_{\phi n}.$$

In order to retain overall vertical equilibrium of the shell, it is sufficient to consider the transverse shearing stresses q_ϕ distributed in a like manner as the meridional stress. For the solution of the loading case represented by Fig. 3c

$$q_\phi(\phi_s) = \sum_{n=2}^{\infty} \bar{q}''_{\phi n}(\phi_s) \cos n\theta, \tag{16}$$

in which $\bar{q}''_{\phi n}(\phi_s) = \bar{q}'_{\phi n} - \bar{q}_{\phi n}$,

$\bar{q}_{\phi n}$ = the transverse shearing stress for harmonic n obtained from the continuous boundary analysis,

and $\bar{q}'_{\phi n}$ is computed by using $\bar{q}_{\phi n}$ in Eq. (13) and then evaluating Eq. (14).

Boundary Conditions

At the base of the shell

$$n_{\phi n} = n''_{\phi n}, \qquad q_{\phi n} = q''_{\phi n}. \tag{17}$$

The ring beam will be assumed to be rigid circumferentially, and also to restrain movement in the horizontal plane. These kinematic conditions

$$V = 0, \qquad U\cos\phi_s + W\sin\phi_s = 0, \tag{18}$$

in which U, V and W are the meridional, circumferential and radial displacements respectively, may be expressed in terms of the stress resultants using the strain-displacement and stress resultant-strain relationships as

$$\epsilon_{\theta n} = n_{\theta n} - \mu n_{\phi n} = 0, \tag{19}$$

in which $\epsilon_{\theta n}$ represents the circumferential strain for harmonic n.

The base will be assumed to be unrestrained against rotation about the circumference so that

$$m_{\phi n} = 0. \tag{20}$$

The top of the shell is assumed to be stress free, i. e.,

$$n_{\phi n} = 0, \qquad q^*_{\phi n} = 0, \qquad n^*_{\theta\phi n} = 0, \qquad m_{\phi n} = 0, \tag{21}$$

in which $n^*_{\theta\phi n} = n_{\theta\phi n} + \dfrac{m_{\theta\phi n}}{r_\theta}$ and $q^*_{\phi n} = q_{\phi n} + \dfrac{n}{r_\theta \sin\phi} m_{\theta\phi n}$.

Numerical Analysis

A typical hyperboloid, defined by $a/s = 0.55$, $a/t = 0.90$, $k^2 = 1.18$, $c = 30$, $\Omega = 0.021$ and $h = 0.00712$, will be considered to illustrate the behavior of the various stress resultants. These values correspond to an actual shell with a 6 in. thickness and 140 ft. throat diameter. The design wind pressure, P_r, is taken as unity for purposes of comparison. Such a shell with a continuous boundary has been studied elsewhere [5], [6], [8]. In the following figures, only the stress resultants due to the design wind pressure are shown. It should be noted that for actual shells, the stresses due to dead load must be added to obtain the net effect of the combined loading. Since a small variation in design

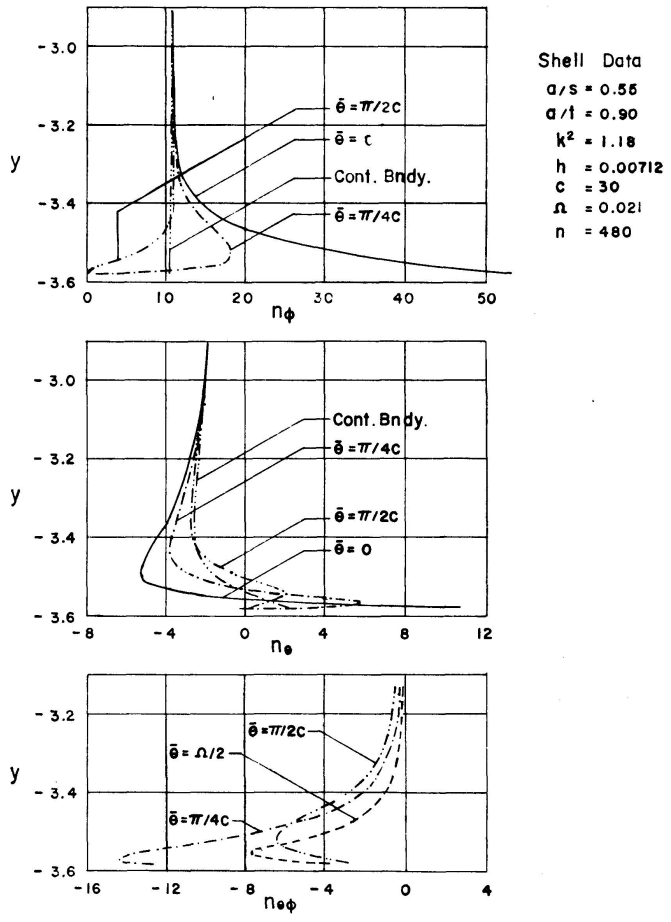

Fig. 4. Membrane Stress Resultants – Circumferential Variation $\theta = 0°$.

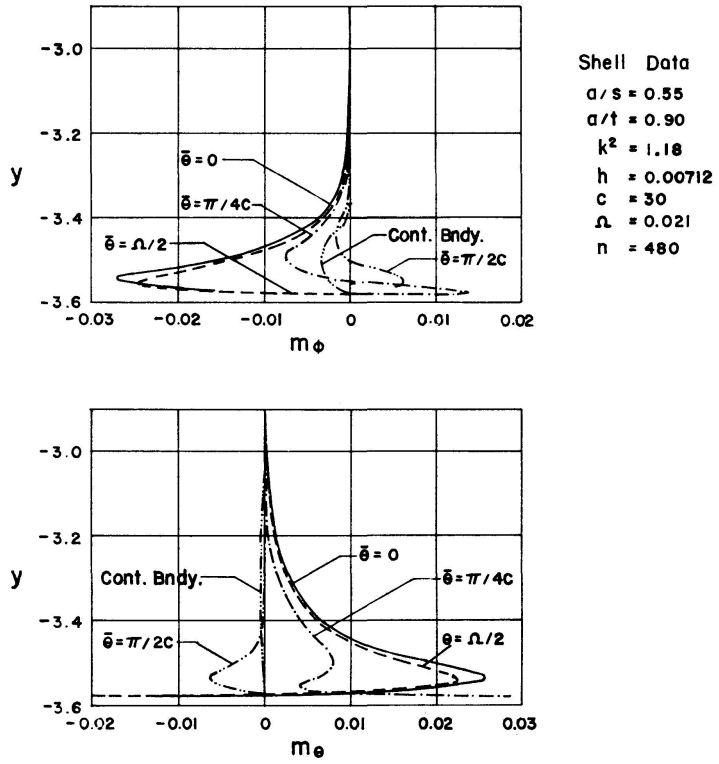

Fig. 5. Bending Stress Resultants – Circumferential Variation $\theta = 0°$.

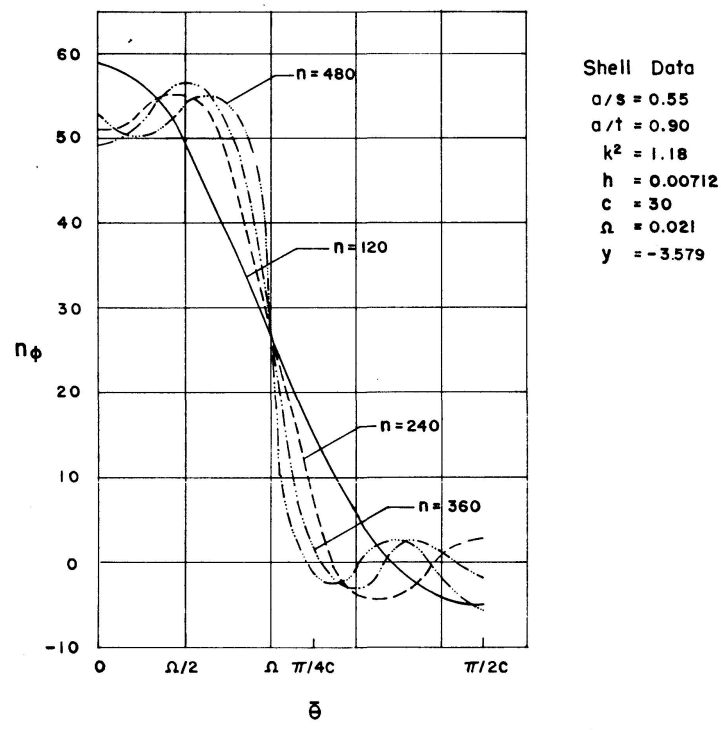

Fig. 6. Convergence of n_θ at the Base of the Shell $\theta = 0°$.

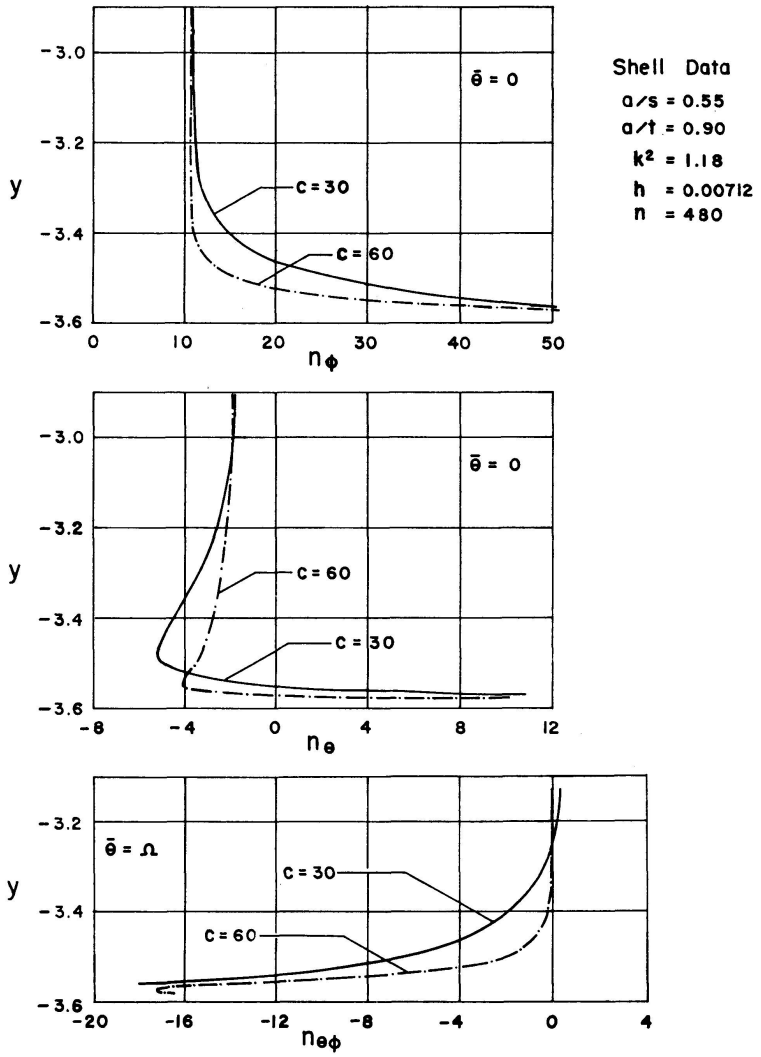

Fig. 7. Membrane Stress Resultants – Effect of Column Spacing $\theta = 0°$.

wind load can cause a very large change in the tension in the vicinity of the windward column, it is recommended that an ultimate strength approach with appropriate load factors for the combination of dead and wind loading be used. Recommendations for suitable load factors and material safety coefficients have been made by PADUART [9].

In Figs. 4 and 5 values of the total stress resultants, as computed from superposition analysis shown in Fig. 3, are plotted against arguments of y. Also shown are the values of n_ϕ, n_θ, $n_{\theta\phi}$, m_ϕ, and m_θ obtained from a continuous boundary analysis. Results are shown only for the windward column with centerline at $\theta = 0°$. The corresponding results for the column with the maximum compressive reaction show similar trends but are generally opposite in sense.

Although ϕ was used as the independent variable in the previously derived expressions, the vertical coordinate y is preferable for illustrating the meri-

dional variation of the stress resultants. For this shell the base corresponds to $y = -3.579$. The coordinates $\bar{\theta} = 0$, $\Omega/2$, $\pi/4c$ and $\pi/2c$ indicate respectively, the column center line, the column quarter point, and the eighth and quarter points of the arc between column center lines measured in the direction of increasing θ. The series given by Eq. (5b) are truncated after 480 terms where the remaining terms are less than 1% of the partial sum. In the interest of computational expedience, harmonics with Fourier coefficients $\bar{n}'_{\phi n}$ less than 1% of $\bar{R}_0$ are neglected. It is apparent from Figs. 4 and 5 that consideration of the discrete support system results in a significant magnification of both the in-plane and bending stress over those computed from a continuous boundary analysis. The intensification of the stress resultants dissipates rapidly away from the base of the shell corroborating the basic assumption used in deriving Eq. (6).

Fig. 6 illustrates the convergence of the Fourier series given by Eq. (15) describing the boundary system shown in Fig. 3. The truncation of the series at $n = 480$, of course, provides the best representation but the greatest improvement is obtained in increasing n from 120 to 240.

The effect of altering the spacing of the columns is illustrated in Figs. 7 and 8. Values of $c = 30$ and 60 are plotted. For $c = 60$ the column width is halved so that the value of n_ϕ at the base of the shell is the same in both cases. Increasing the number of column is seen to be beneficial, in general, since the

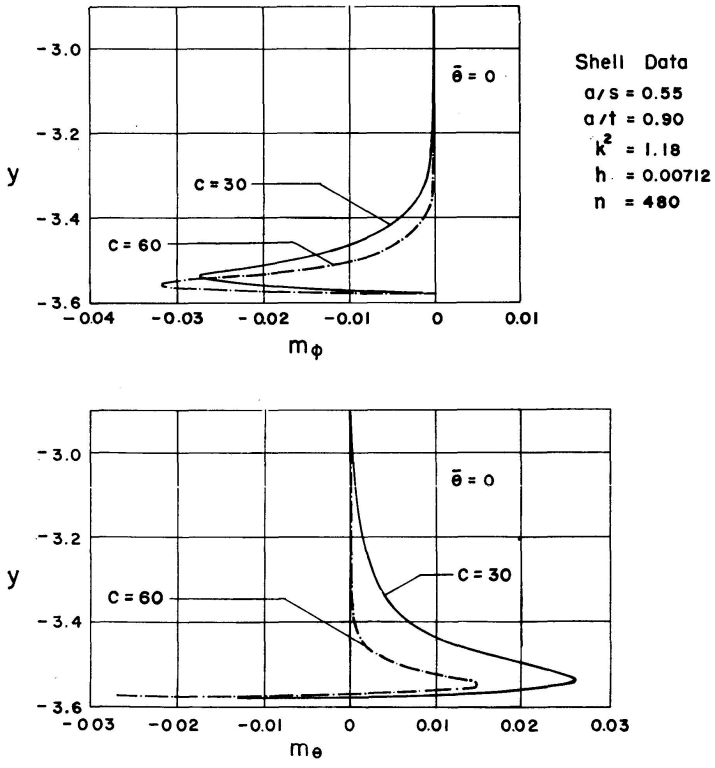

Fig. 8. Bending Stress Resultants – Effect of Column Spacing $\theta = 0°$.

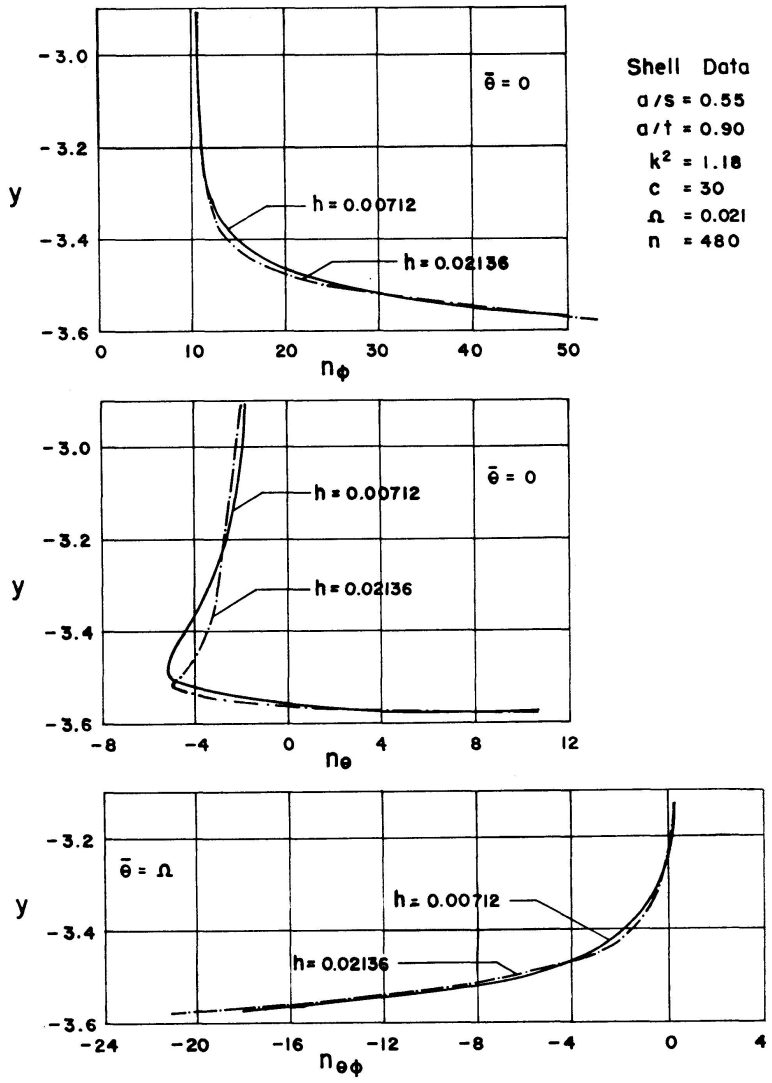

Fig. 9. Membrane Stress Resultants – Effect of Shell Thickness $\theta = 0°$.

amplification of the stress resultants due to the discrete supports is reduced in all cases except for the meridional bending moment.

To provide increased resistance for the comparatively large bending stresses in the vicinity of the base of the shell, the thickness is often increased. The analysis of shells with variable thickness is beyond the scope of this investigation; however, since the column effects are greatest in the immediate region of the base of the shell, it is felt that taking the value of H as the base thickness in the current analysis provides a good approximation. In Figs. 9 and 10, the stress resultants are shown to be increased only slightly while the shell in-plane and bending capacities are increased many times so that increasing the thickness at the base of the shell is apparently an efficient means of dealing with the local effects of the discrete support systems.

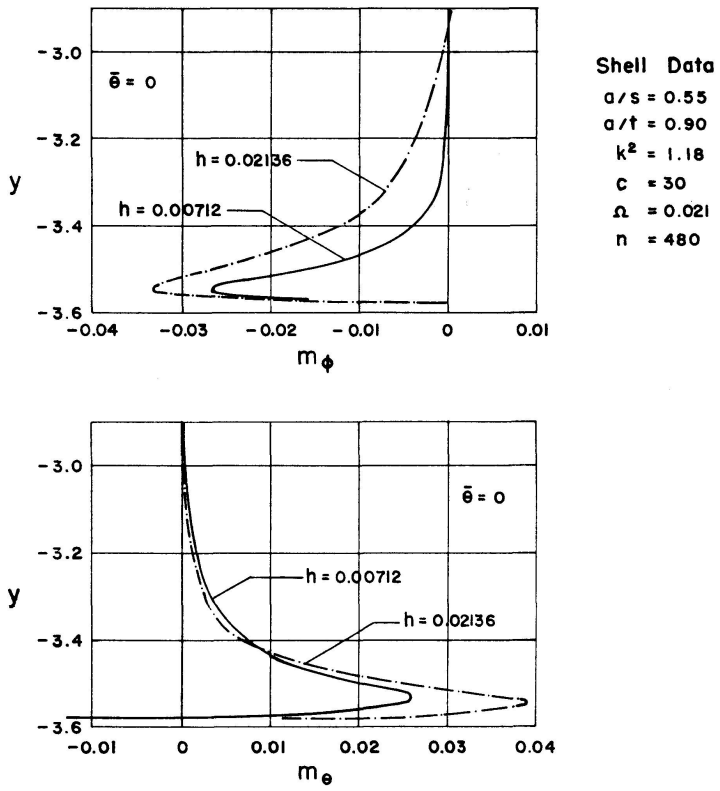

Fig. 10. Bending Stress Resultants – Effect of Shell Thickness $\theta = 0°$.

Conclusions

Considering the homogeneous part of the governing equations of the bending theory of shells of revolution in complex form and introducing certain geometrical approximations based on the geometry of the hyperboloid and the supposition of rapidly attenuating edge effects facilitates the derivation of explicit expressions for the in-plane and bending stress resultants for a general harmonic loading. Using the results of a continuous boundary analysis together with the derived homogeneous solution, the column-supported boundary is represented in idealized form by assuming the column reactions to be uniform under the action of a quasistatic design wind load.

For a shell with representative dimensions, both the in-plane and bending stresses are increased significantly over those values computed considering a continuous boundary. Using a greater number of columns to provide a given total support width reduces the magnitude of the amplification of the stress resultants. Also, local thickening in the region of the shell boundary appears to be an effective way of providing increased resistance against the comparatively large stress resultants in the vicinity of the base of the shell.

Acknowledgement

The research upon which this paper is based was supported by the National Science Foundation under Grant GK-1501 to Washington University. The general assistance of the Washington University Computation Center is also appreciated.

Appendix I. Explicit Expressions for Stress Resultants

$$[D_1] = [\beta_6 \beta_6 \beta_8 \beta_8 \beta_5 \beta_5 \beta_7 \beta_7]_{8\times 8}, \tag{22}$$

$[D_2] =$

$$\begin{bmatrix}
\alpha_2 & -\alpha_1 & \alpha_1 & \alpha_2 & \alpha_2 & -\alpha_1 & \alpha_1 & \alpha_2 & -\alpha_3 & -\alpha_1 & \alpha_1 & -\alpha_3 & -\alpha_3 & -\alpha_1 & \alpha_1 & -\alpha_3 \\
-\alpha_1 & -\alpha_2 & \alpha_2 & -\alpha_1 & -\alpha_1 & -\alpha_2 & \alpha_2 & -\alpha_1 & -\alpha_1 & \alpha_3 & -\alpha_3 & -\alpha_1 & -\alpha_1 & \alpha_3 & -\alpha_3 & -\alpha_1 \\
1 & 0 & 0 & 1 & 1 & 0 & 0 & 1 & -1 & 0 & 0 & -1 & -1 & 0 & 0 & -1 \\
0 & -1 & 1 & 0 & 0 & -1 & 1 & 0 & 0 & 1 & -1 & 0 & 0 & 1 & -1 & 0 \\
\alpha_5 & \alpha_6 & -\alpha_6 & \alpha_5 & \alpha_7 & -\alpha_8 & \alpha_8 & \alpha_7 & -\alpha_9 & -\alpha_{10} & \alpha_{10} & -\alpha_9 & -\alpha_{11} & \alpha_{12} & -\alpha_{12} & -\alpha_{11} \\
\alpha_6 & -\alpha_5 & \alpha_5 & \alpha_6 & -\alpha_8 & -\alpha_7 & \alpha_7 & -\alpha_8 & -\alpha_{10} & \alpha_9 & -\alpha_9 & -\alpha_{10} & \alpha_{12} & \alpha_{11} & -\alpha_{11} & \alpha_{12} \\
\alpha_{13} & \alpha_{14} & -\alpha_{14} & \alpha_{13} & \alpha_{15} & -\alpha_{16} & \alpha_{16} & \alpha_{15} & -\alpha_{17} & -\alpha_{18} & \alpha_{18} & -\alpha_{17} & -\alpha_{19} & \alpha_{20} & -\alpha_{20} & -\alpha_{19} \\
\alpha_{14} & -\alpha_{13} & \alpha_{13} & \alpha_{14} & -\alpha_{16} & -\alpha_{15} & \alpha_{15} & -\alpha_{16} & -\alpha_{18} & \alpha_{17} & -\alpha_{17} & -\alpha_{18} & \alpha_{20} & \alpha_{19} & -\alpha_{19} & \alpha_{20}
\end{bmatrix}_{8\times 16}, \tag{23}$$

$[\bar{U}] =$

$$\begin{bmatrix}
\beta_{21}\cos\beta_{25} & 0 & 0 & 0 & 0 & 0 & 0 & 0 \\
\beta_{21}\sin\beta_{25} & 0 & 0 & 0 & 0 & 0 & 0 & 0 \\
0 & \beta_{21}\cos\beta_{25} & 0 & 0 & 0 & 0 & 0 & 0 \\
0 & \beta_{21}\sin\beta_{25} & 0 & 0 & 0 & 0 & 0 & 0 \\
0 & 0 & \beta_{22}\cos\beta_{26} & 0 & 0 & 0 & 0 & 0 \\
0 & 0 & \beta_{22}\sin\beta_{26} & 0 & 0 & 0 & 0 & 0 \\
0 & 0 & 0 & \beta_{22}\cos\beta_{26} & 0 & 0 & 0 & 0 \\
0 & 0 & 0 & \beta_{22}\sin\beta_{26} & 0 & 0 & 0 & 0 \\
0 & 0 & 0 & 0 & \beta_{23}\cos\beta_{27} & 0 & 0 & 0 \\
0 & 0 & 0 & 0 & \beta_{23}\sin\beta_{27} & 0 & 0 & 0 \\
0 & 0 & 0 & 0 & 0 & \beta_{23}\cos\beta_{27} & 0 & 0 \\
0 & 0 & 0 & 0 & 0 & \beta_{23}\sin\beta_{27} & 0 & 0 \\
0 & 0 & 0 & 0 & 0 & 0 & \beta_{24}\cos\beta_{28} & 0 \\
0 & 0 & 0 & 0 & 0 & 0 & \beta_{24}\sin\beta_{28} & 0 \\
0 & 0 & 0 & 0 & 0 & 0 & 0 & \beta_{24}\cos\beta_{28} \\
0 & 0 & 0 & 0 & 0 & 0 & 0 & \beta_{24}\sin\beta_{28}
\end{bmatrix}_{16\times 8}, \tag{24}$$

$$[B] =$$

$$\begin{bmatrix}
\frac{1}{r_\theta \sin^2\phi} & 0 & 0 & 0 & 0 & 0 & 0 & \frac{-\nu\cot\phi}{r_\phi} \\
\frac{-1}{r_\theta \sin^2\phi} & 0 & 1 & 0 & 0 & 0 & 0 & \frac{\nu\cot\phi}{r_\phi} \\
0 & 0 & 0 & \frac{\cot\phi}{r_\theta \sin\phi} & \frac{-1}{n r_\phi \sin\phi} & 0 & 0 & 0 \\
0 & \frac{\nu(1-\mu)}{r_\theta \sin^2\phi} & 0 & -\nu & 0 & 0 & \frac{\nu(\nu-\mu)\cot\phi}{r_\phi} & 0 \\
0 & \frac{-\nu(1-\mu)}{r_\theta \sin^2\phi} & 0 & -\nu\mu & 0 & 0 & \frac{-\nu(\nu-\mu)\cos\phi}{r_\phi} & 0 \\
0 & 0 & \frac{-n\nu^2(1-\mu)\cos\phi}{r_\theta \sin^2\phi} & 0 & 0 & \frac{-\nu(1-\mu)}{n r_\phi \sin\phi} & 0 & 0 \\
0 & 0 & 0 & 0 & 0 & 0 & 0 & \frac{-\nu}{r_\phi} \\
0 & 0 & 0 & \frac{-n\nu}{r_\theta \sin\phi} & 0 & 0 & 0 & 0
\end{bmatrix}_{8\times 8}, \quad (25)$$

$$\{C\} = \{C_1\, C_2\, C_3\, C_4\, C_5\, C_6\, C_7\, C_8\}, \quad (26)$$

where $C_1 - C_8$ are constants of integration and

$$\gamma_3 = \frac{\gamma_1}{2} + \frac{\Pi}{4}, \qquad \gamma_4 = \frac{\gamma_2}{2} + \frac{\Pi}{4},$$

$$\beta_3 = \frac{\sqrt[4]{r_\theta/\nu}}{r_\theta \sqrt{\sin\phi}}, \qquad \beta_4 = \frac{\beta_3 \cot\phi}{4}\left(1 - \frac{3\, r_\phi}{r_\theta}\right), \qquad \beta_5 = \frac{-1}{2n\sqrt{-\delta}},$$

$$\beta_6 = \beta_3 \beta_5, \qquad \beta_7 = \frac{-\sqrt{-\delta}}{n}, \qquad \beta_8 = \beta_3 \beta_7,$$

$$\beta_9 = \frac{n^2 \nu (r_\phi + r_\theta)\cos\phi\, W_0 \sin\gamma_0}{r_\theta^2 \sin^3\phi}, \qquad \beta_{10} = \frac{2 n^4 \nu^2 (r_\phi + r_\theta)\cos\phi}{r_\theta^3 \sin^5\phi},$$

$$\beta_{11} = \frac{dW_1}{d\phi} = -(\beta_9 + \beta_{10}), \qquad \beta_{12} = \frac{dW_2}{d\phi} = \beta_9 - \beta_{10}, \quad (27)$$

$$\beta_{13} = \frac{1}{4}\frac{d\gamma_1}{d\phi} = \frac{-1}{1+\bar{\gamma}_1^2}\left[\frac{0.5\, n^2 \nu (1 + W_0 \cos\gamma_0)(r_\phi + r_\theta)\sin\phi\cos\phi}{(2 n^2 \nu + r_\theta \sin^2\phi\, W_0 \sin\gamma_0)}\right],$$

$$\beta_{14} = \frac{1}{4}\frac{d\gamma_2}{d\phi} = \frac{-1}{1+\bar{\gamma}_2^2}\left[\frac{0.5\, n^2 \nu (1 + W_0 \cos\gamma_0)(r_\phi + r_\theta)\sin\phi\cos\phi}{(2 n^2 \nu - r_\theta \sin^2\phi\, W_0 \sin\gamma_0)}\right],$$

$$\beta_{15} = \beta_4^4 - \frac{\beta_3 \beta_{11}}{8\, W_1}, \qquad \beta_{16} = \beta_4 - \frac{\beta_3 \beta_{12}}{8\, W_2}, \qquad \beta_{17} = \beta_3 \alpha_4 \cos\gamma_1\, W_1^{0.25},$$

$$\beta_{18} = \beta_3 \alpha_4 \cos\gamma_2\, W_2^{0.25}, \qquad \beta_{19} = \alpha_4 \sin\gamma_1\, W_1^{0.25}, \qquad \beta_{20} = \alpha_4 \sin\gamma_2\, W_2^{0.25},$$

$$\beta_{21} = e^{\beta_{1r}}\, W_1^{-0.125}, \qquad \beta_{22} = e^{-\beta_{1r}}\, W_1^{-0.125}, \qquad \beta_{23} = e^{\beta_{2r}}\, W_2^{-0.125},$$

$$\beta_{24} = e^{-\beta_{2r}}\, W_2^{-0.125}, \qquad \beta_{25} = \gamma_3 - \beta_{1i}, \qquad \beta_{26} = \gamma_3 + \beta_{1i},$$

$$\beta_{27} = \gamma_4 - \beta_{2i}, \qquad \beta_{28} = \gamma_4 + \beta_{2i}, \tag{27}$$

$$\beta_{jr} = \int_{\phi_t}^{\phi} Re\, F_j\, d\phi, \qquad \beta_{ji} = \int_{\phi_t}^{\phi} Im\, F_j\, d\phi, \qquad \bar{\beta}_{jr} = \int_{\phi_s}^{\phi} Re\, F_j\, d\phi, \qquad (j = 1, 2),$$

$$\begin{aligned}
&\alpha_1 = n\sqrt{-2\nu\delta}, && \alpha_2 = 1-\alpha_1, && \alpha_3 = 1+\alpha_1,\\
&\alpha_4 = \frac{r_\phi}{\sqrt{r_\theta \nu}}, && \alpha_5 = \alpha_2\alpha_{13}+\alpha_1\alpha_{14}, && \alpha_6 = \alpha_2\alpha_{14}-\alpha_1\alpha_{13},\\
&\alpha_7 = \alpha_2\alpha_{15}-\alpha_1\alpha_{16}, && \alpha_8 = \alpha_2\alpha_{16}+\alpha_1\alpha_{15}, && \alpha_9 = \alpha_3\alpha_{17}-\alpha_1\alpha_{18},\\
&\alpha_{10} = \alpha_3\alpha_{18}+\alpha_1\alpha_{17}, && \alpha_{11} = \alpha_3\alpha_{19}+\alpha_1\alpha_{20}, && \alpha_{12} = \alpha_3\alpha_{20}-\alpha_1\alpha_{19},\\
&\alpha_{13} = \beta_{15}-\beta_{17}, && \alpha_{14} = \beta_3(\beta_{13}+\beta_{19}), && \alpha_{15} = \beta_{15}+\beta_{17},\\
&\alpha_{16} = \beta_3(\beta_{13}-\beta_{19}), && \alpha_{17} = \beta_{16}-\beta_{18}, && \alpha_{18} = \beta_3(\beta_{14}+\beta_{20}),\\
&\alpha_{19} = \beta_{16}+\beta_{18}, && \alpha_{20} = \beta_3(\beta_{14}-\beta_{20}).
\end{aligned} \tag{28}$$

Appendix II. Notation

a	throat radius
b	shell parameter defined by Eq. (1b)
c	total number of column support points
$C_1 - C_8$	integration constants
$\tilde{C}_{1j}$, $\tilde{C}_{2j}$	complex integration constants
$[D_1]$ $[D_2]$	matrices defined by Eqs. (22) and (23)
F_j	variable defined in Eq. (17)
h, H	shell thickness
j	index designation (1 or 2)
k	shell parameter defined by Eq. (1b)
m_ϕ, m_θ, $m_{\theta\phi}$, $m_{\phi\theta}$	nondimensional moment resultants
$m_{\phi n}$, $m_{\theta n}$, $m_{\theta\phi n}$	m_ϕ, m_θ, $m_{\theta\phi}$ for harmonic n
M_ϕ, M_θ, $M_{\theta\phi}$, $M_{\phi\theta}$	moment resultants
n	harmonic number
n_ϕ, n_θ, $n_{\theta\phi}$, $n_{\phi\theta}$	nondimensional stress resultants
$n_{\phi n}$, $n_{\theta n}$, $n_{\theta\phi n}$	n_ϕ, n_θ, $n_{\theta\phi}$ for harmonic n
$\bar{n}'_{\phi n}$, $\bar{n}''_{\phi n}$	coefficients defined by Eqs. (14) and (15)
$n^*_{\theta\phi n}$	effective membrane shear
N_ϕ, N_θ, $N_{\theta\phi}$, $N_{\phi\theta}$	stress resultants
P_r	reference design wind pressure
q_ϕ, q_θ	nondimensional transverse shearing stress resultants
$q_{\phi n}$, $q_{\theta n}$	q_ϕ, q_θ for harmonic n
$\bar{q}'_{\phi n}$, $\bar{q}''_{\theta n}$	coefficients defined by Eq. (16)
$q^*_{\phi n}$	effective meridional transverse shear
Q_ϕ, Q_θ	transverse shearing stress resultants
r_ϕ, r_θ, r_0	nondimensional radii of curvature

$\{R\}, \{R_n\}$	vectors defined by Eq. (5)
$\bar{R}_\lambda$	column reaction
R_0, R_ϕ, R_θ	radii of curvature
s	base radius
S	vertical distance from throat to base of shell
t	top radius
T	vertical distance from throat to top of shell
$[\bar{U}]$	matrix defined by Eq. (23)
U, V, W	displacements
y, Y	vertical coordinate
$\alpha_1 - \alpha_{20}$	variables defined by Eq. (28)
β_j	variables defined by Eq. (9)
$\beta_3 - \beta_{28}$	variables defined by Eq. (27)
$\beta_{jr}, \beta_{ji}, \bar{\beta}_{jr}$	variables defined by Eq. (27)
γ_3, γ_4	variables defined by Eq. (27)
δ	parameter defined by Eqs. (3), (4), and (6)
$\epsilon_{\theta n}$	circumferential strain for harmonic n
$\theta, \bar{\theta}, \theta_\lambda$	circumferential coordinates
λ	column number
μ	Poisson's ratio
ν	parameter defined in Eq. (7)
ϕ	meridional coordinate
ϕ_s, ϕ_t	angle locating base and top of shell
Ω	angle in horizontal plane subtended by half width of a column

Appendix III. References

1. Elms, D. G.: Shells of Revolution with Concentrated Edge Forces. Journal of the Engineering Mechanics Division, ASCE, Vol. 95, No. EM 3, Proc. Paper 6625, June, 1969, pp. 711–730.
2. Flugge, W.: Stresses in Shells. Springer-Verlag, Berlin, 1962, pp. 53–58, 234–237.
3. Gould, P. L. and Lee, S. L.: Bending of Hyperbolic Cooling Towers. Journal of the Structural Division, ASCE, Vol. 93, No. ST 5, October, 1967, pp. 125–146.
4. Gould, P. L.: Unsymmetrically Loaded Hyperboloids of Revolution. Journal of the Engineering Mechanics Division, ASCE, Vol. 94, No. EM 4, October, 1968, pp. 1029–1043.
5. Gould, P. L. and Lee, S. L.: Hyperboloids of Revolution Supported on Columns. Journal of the Engineering Mechanics Division, ASCE, Vol. 95, No. EM 5, October, 1969, pp. 1083–1100.
6. Lee, S. L. and Gould, P. L.: Hyperbolic Cooling Towers Under Wind Load. Journal of the Structural Division, ASCE, Vol. 93, No. ST 5, October, 1967, pp. 487–514.
7. Nieman, H. J.: Wind Pressure Measurements on Cooling Towers. Proceedings of the Conference on Tower-Shaped Structures, International Association for Shell Structures, April, 1969.

8. NOVOZHILOV, V. V.: Thin Shell Theory. Trans. from Russian 2nd ed., P. Noordhoff, Ltd., Groningen, The Netherlands, 1959, pp. 303, 315–326, 377–385.
9. PADUART, A.: On Problems of Cooling Towers. Bulletin of the International Association for Shell Structures, No. 36, December, 1968, pp. 45–50.
10. RISH, R. F. and STEEL, R. F.: Design and Selection of Hyperbolic Cooling Towers. Journal of the Power Division, ASCE, Vol. 85, No. PO 5, Proc. Paper 2227, October, 1959, pp. 89–117.
11. STEELE, C. R.: Shells of Revolution with Edge Loads of Rapid Circumferential Variation. Journal of Applied Mechanics, ASME, December, 1962, pp. 701–707

Summary

The governing homogeneous equations of the bending theory of thin shells of revolution are solved for a hyperboloid of revolution in a form suitable for representing a column-supported boundary. For a quasistatic design wind loading, a superposition representation is used to derive a set of explicit expressions for the stress resultants. The data presented indicates that the consideration of the discrete support system in the analysis, rather than the idealized continuous boundary, results in an increase in stresses in the vicinity of the base of the shell.

Résumé

Les équations homogènes déterminantes de la théorie de flexion pour voiles minces de révolution sont résolues pour un hyperboloide de révolution, dans une forme appropriée pour la représentation d'une limite appuyée sur des colonnes. Pour une distribution de charges du vent quasiment statique, une représentation de superposition nous permet de dériver un ensemble d'expressions qui fournissent la résultante des charges. Les données présentées indiquent que considérer l'analyse d'un système de supports rapprochés, plutôt qu'une limite idéalisée et continue, entraîne un accroissement des solliciatations dans la région de la base du voile.

Zusammenfassung

Die bestimmenden homogenen Gleichungen der Biegungstheorie dünner Rotationsschalen werden für ein Rotationshyperboloid in einer, für die Darstellung einer durch Stützen getragenen Randlinie, geeigneten Form gelöst. Für eine gewissermassen statische Windbelastung wird eine Überlagerungsdarstellung benutzt, um eine Gruppe bestimmter Ausdrücke für die Belastungs-Resultierenden abzuleiten. Die dargestellten Daten zeigen, dass die Betrachtung des unstetigen Tragsystems in der Analyse, eher als die idealisierte kontinuierliche Randlinie, in einem Anwachsen der Beanspruchungen in der Nähe der Schalenbasis zum Ausdruck kommt.